SCREENING OF THE QCD HEAVY QUARK POTENTIAL AT FINITE TEMPERATURE

F. KARSCH
Theory Division, CERN, CH-1211 Geneva 23, Switzerland

and

H.W. WYLD
Department of Physics, University of Illinois at Urbana-Champaign, 1110 West Green Street, Urbana, IL 61801, USA

Received 18 July 1988

We study the heavy quark potential for two-flavour QCD in the high-temperature chiral symmetric phase. The potential between static fermion sources has been calculated in the presence of light quarks of mass $m/T=0.1$ on lattices of size $12^3 4$ and $8^3 4$. We find a significant increase in the screening mass over that in the pure SU(3) gauge theory. We also have analyzed the rotational symmetry of the potential and the influence of finite-lattice-size effects on the potential and other thermodynamic observables.

It is generally expected that static colour charges are screened in the high-temperature chiral symmetric phase of QCD. This expectation is based on a perturbative analysis of the high-temperature phase which shows that the colour averaged static quark–anti-quark potential is of the form

$$V(r, T) \simeq -(1/r^d) \exp(-\mu r) , \qquad (1)$$

with $d=2$ and screening mass $\mu=2m_D$. Here

$$m_D^2(T) = (\tfrac{1}{3}N+\tfrac{1}{6}n_f)g^2(T)T^2 \qquad (2)$$

is the perturbative result for the Debye screening mass (inverse screening length) in an SU(N) gauge theory with n_f massless fermions and $g(T)$ denotes the temperature dependent running coupling constant. This perturbative approach, however, is questionable as higher order corrections are not calculable systematically [1].

Within the framework of lattice Monte Carlo simulations a non-perturbative analysis of the heavy quark potential is possible. For the pure SU(N) gauge theories one finds that the screening length is rather small even close to the chiral phase transition (in general for $T/T_c \geqslant 1.2$) [2–5]. First simulations for QCD [6] indicate that the screening length becomes even smaller in the presence of dynamical quarks, as expected from eq. (2). This is a rather exciting result as it opens the possibility that the melting of heavy quark resonances may happen already at temperatures close to T_c [7,8] and thus may provide a signal for quark–gluon plasma formation [7].

For a quantitative discussion of heavy quark bound state formation in the quark–gluon plasma a detailed analysis of the functional form of the potential at intermediate distances, $rT \leqslant 1$, is of importance. In contrast to this the determination of the Debye screening length requires an analysis of the large-distance behaviour of the potential. Already in the pure gauge sector it turned out to be difficult to measure the potential at distances $rT \geqslant 1.5$ [4,5]. It will be even more so in the presence of light dynamical quarks. Given the present status of fermion algorithms we cannot expect to gather more statistics than in the pure gauge sector, so we will not gain much information about the potential at large distances. We can, however, analyze the intermediate distance properties and compare with corresponding results in the pure gauge sector. In the following we will present such an analysis for QCD with two light flavours.

The numerical simulation has been performed with a hybrid microcanonical Langevin algorithm [9] for noisy staggered fermions which has been improved

according to the scheme developed by Gottlieb et al. [10]. Thus for our simulation with two light flavours the error in physical observables is only $O(d\tau^2)$. All our calculations have been performed on lattices of size $N_\sigma^3 N_\tau$ with $N_\tau = 4$ and quark masses $ma = 0.025$. We have used a small discrete time step for the integration of the differential equations [9,10]; $d\tau = 0.01$ on the $12^3 4$ lattice and $d\tau = 0.02$ on the $8^3 4$ lattice. We have compared our algorithm on small lattices with results of ref. [10] and find in general good agreement. A quite sensitive consistency check is the determination of β_c for small quark masses. In fig. 1 we show the evolution of the Polyakov loop at $\beta =$ 5.28, 5.29 and 5.30 on an $8^3 4$ lattice at quark mass $ma = 0.025$: The starting configuration is a well equilibrated configuration at $\beta = 5.3$. From this we switched to $\beta = 5.28$ at Monte Carlo time $\tau = 900$ and then to $\beta = 5.29$ at $\tau = 1600$. From these runs we conclude that the critical coupling is $\beta = 5.29 \pm 0.005$ in good agreement with the value $\beta_c = 5.2875 \pm 0.0025$ quoted in refs. [11,12].

We determine the potential from Polyakov loop correlation functions as

$$\exp[-V(\boldsymbol{r}, T)/T] = \frac{\langle \mathrm{Tr}\, L(0)\, \mathrm{Tr}\, L^\dagger(\boldsymbol{r}) \rangle}{\langle |L| \rangle^2} . \qquad (3)$$

Here $\boldsymbol{x} = \boldsymbol{r}/a$ is the spatial separation measured in lattice units, a, and

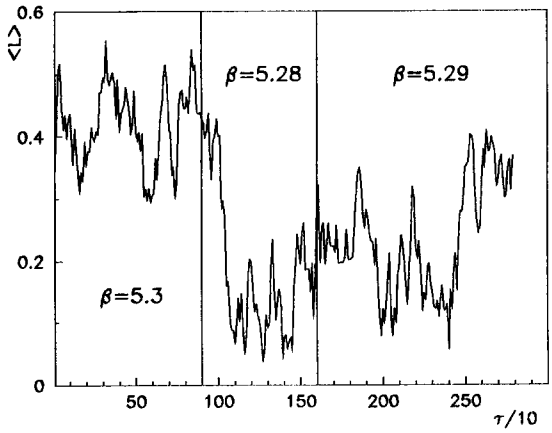

Fig. 1. Evolution of the Polyakov loop expectation value with Monte Carlo time on an $8^3 4$ lattice for two quark flavours of mass $ma = 0.025$ at $\beta = 5.28$ and 5.29. As starting configuration an equilibrated configuration at $\beta = 5.3$ has been used.

$$L = \frac{1}{N_\sigma^3} \sum_{\boldsymbol{x}} \mathrm{Tr}\, L(\boldsymbol{x}) \qquad (4)$$

is the average Polyakov loop measured on a lattice of size $N_\sigma^2 N_\tau$. Besides the usual correlations between on-axis Polyakov loops we also calculated correlations between off-axis loops. This allows us to study the rotational symmetry of the potential [13]. In addition it improves somewhat our statistics and fits although the correlation functions at different separations are highly correlated.

From the analysis of finite-size effects in the pure gauge sector [5] we know that a large asymmetry in the spatial and temporal lattice size is needed to get a reasonable approximation to the infinite-volume potential even for intermediate distances between the sources. Our simulations have been performed on a $12^3 4$ lattice. Due to the spatial periodic boundary conditions the potential is periodic around $rT = N_\sigma/2N_\tau$. The largest distance we can reach on this lattice is thus $rT = 1.5$. We have selected four different couplings for our simulations, $\beta = 5.3$, 5.4, 5.6 and 5.8. Previous simulations of two-flavour QCD with the same quark mass have shown evidence for a first-order chiral phase transition at $\beta_c = 5.2875(25)$ [11,12] and at $\beta_c = 5.438(40)$ [12] on lattices with $N_\tau = 4$ and 6, respectively. The change in β needed to increase the lattice cut-off by a factor 1.5 ($\Delta\beta \simeq 0.15$) is thus about a factor 2 smaller than expected in the asymptotic scaling regime. Similar violations of asymptotic scaling have been observed in the pure gauge sector at intermediate values of β. Taking these scaling violations into account we can estimate the temperatures that correspond to our choice of couplings; we find $T/T_c \simeq 1.1$, 1.4, 2.0 and 3.0. This covers the temperature range which is most important for the phenomenological analysis of the heavy quark potential [7,8].

In order to measure the potential on the $12^3 4$ lattice we performed at each β-value about 50 000 iterations, taking measurements every tenth iteration. The error analysis turned out to be rather difficult as the measurements of the denominator and numerator in eq. (3) are highly correlated. Taking the error one obtains for both quantities as independent clearly is an overestimate. On the other hand we do not have enough data to perform a detailed error analysis on subsamples of varying size. In order to estimate the

error we arbitrarily divided our data sample into four different blocks, calculated the potential on each block separately and finally determined the error from the spread of these four individual measurements. Results are shown in figs. 2a–2d as a function of the dimensionless variable $rT = |\boldsymbol{x}|/N_\tau$.

At $\beta = 5.3$ and 5.6 we repeated the analysis also on an $8^3 4$ lattice to check finite-size effects. As can be seen in figs. 2a and 2d the potential is somewhat flatter on the $8^3 4$ lattice (it is periodic around $rT = 1$). This is in accordance with the behaviour found for the SU(2) potential [5]. Our results thus suggest that finite lattice effects tend to lower the screening mass even quite close to T_c. This behaviour is opposite to that of finite-size effects found for instance in the analysis of hadron masses. It is, however, in agree-

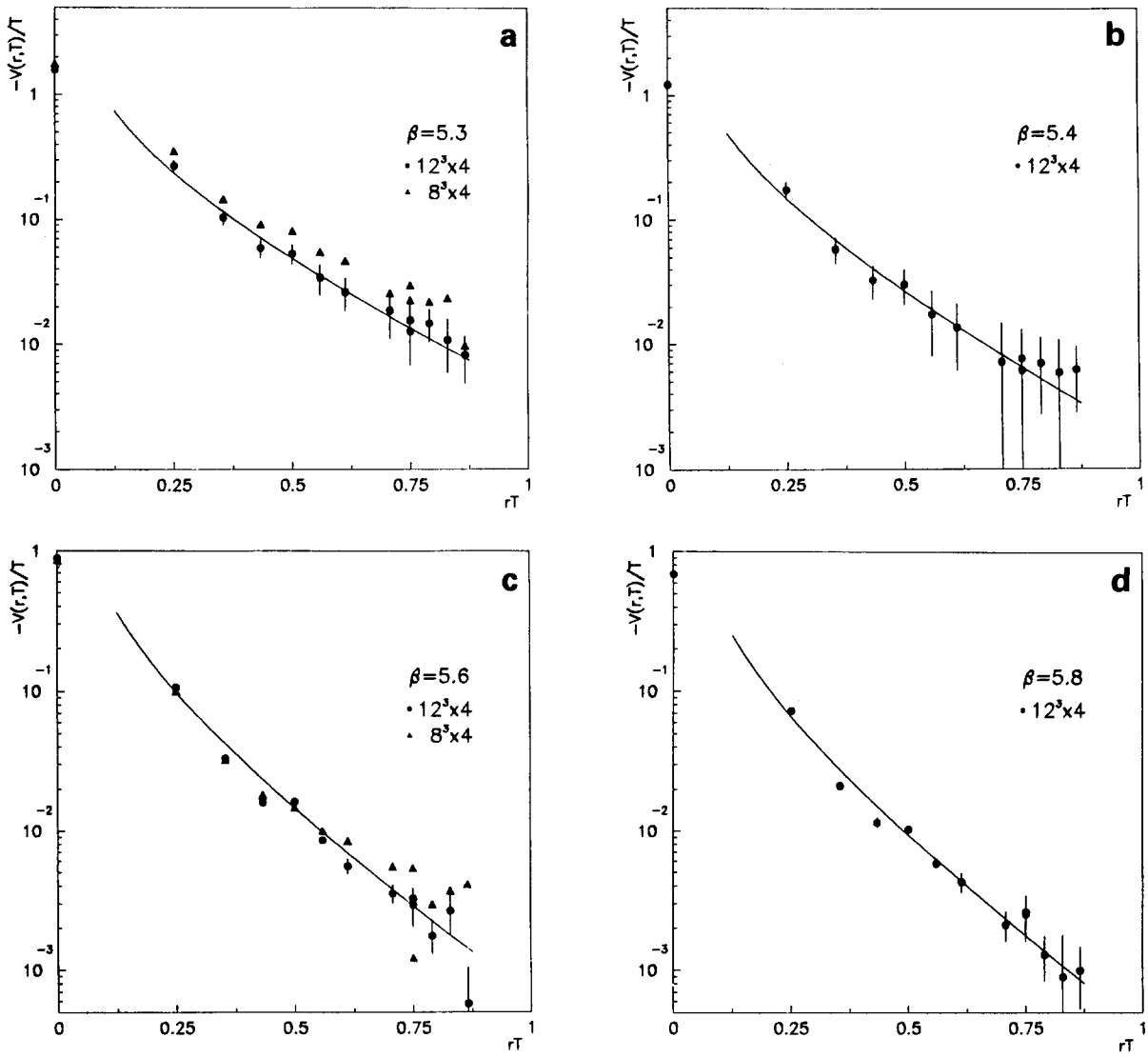

Fig. 2. The heavy quark potential $-V(r, T)/T$ versus rT, $r \equiv |\boldsymbol{r}|$, at $\beta = 5.3$ (a), 5.4 (b), 5.6 (c) and 5.8 (d). Shown are results obtained on a $12^3 4$ lattice (●). For $\beta = 5.3$ and 5.6 we also show results from a simulation on an $8^3 4$ lattice (▲). Error bars are only shown for the $12^3 4$ data. The curves show fits with the continuum form of the potential given in eq. (5).

ment with the perturbative behaviour of the Debye mass in finite volumes [14].

In fig. 2 we also show fits based on the ansatz

$$-V_c(\boldsymbol{r}, T)/T = [\alpha(T)/rT] \exp(-\mu r) , \qquad (5)$$

$r \equiv |\boldsymbol{r}|$. The analysis of the functional form of the potential in the pure gauge sector [4,5] suggests that it would be more appropriate to allow for an arbitrary power d of the Coulomb term in eq. (5) (see eq. (1)). There it has been found that d is close to 1 for temperatures T close to T_c. Only at rather large temperatures does it approach $d=2$ as expected from high-temperature perturbation theory. With the present accuracy of our data it is, however, impossible to perform such a detailed analysis of the functional form of the potential for full QCD. We thus use the simpler two-parameter ansatz given in eq. (5) [#1].

The potentials presented in figs. 2a–2d clearly show that rotational symmetry is not well restored on this size lattice. For instance we find that in all simulations the potential measured along a space diagonal at distance $\sqrt{3}$ is as big as the potential measured "on-axis" at distance 2. The fact that we observe the same pattern of violation of rotational symmetry for all couplings and different lattice sizes also gives us some confidence that our error estimates are reasonable. We thus have analyzed the data both with the continuum form of a Debye screened Coulomb potential given in eq. (5) and with the corresponding lattice form

$$\begin{aligned} -V_L(\boldsymbol{r}, T)/T &= N_\tau \alpha(T) \frac{4\pi}{N_\sigma^3} \sum_{\boldsymbol{p}} [\cos(\boldsymbol{p}\cdot\boldsymbol{x})\{(\mu a)^2 \\ &+ 4[\sin^2(\tfrac{1}{2}p_1) + \sin^2(\tfrac{1}{2}p_2) + \sin^2(\tfrac{1}{2}p_3)]\}^{-1}] , \\ p_i &= n_i 2\pi/N_\sigma , \quad n_i = 0, 1, 2, ..., N_\sigma - 1 , \\ i &= 1, 2, 3 . \end{aligned} \qquad (6)$$

As can be seen from table 1 both fits give similar results for the coupling constant $\alpha(T)$ and the screening mass $\mu(T)$. These numbers agree also quite well with those obtained for three-flavour QCD with quark masses $m/T = 0.4$ [6].

A comparison of both fits is shown in fig. 3. We find that the discrete lattice potential gives a better description of the short-distance part of the potential. In particular it incorporates the faster rise of the potential in off-axis directions. This is reflected in the larger Debye screening mass obtained from the lattice fit at $\beta = 5.6$ and 5.8. A larger temporal lattice size is needed to remove these lattice artifacts from the potential.

With our present statistics we can measure the potential only for distances $rT < 1$. The screening mass extracted from the fits thus should be understood as an effective screening mass describing the short-distance behaviour of the potential. In order to get some idea about the asymptotic screening mass defined at large distances we have considered also effective

Table 1
Coupling constant $\alpha(T)$ and screening mass $\mu(T)$ as obtained from χ^2-fits to the data between $R=1.0$ and $R=3.5$.

β	Continuum fit		Lattice fit	
	$\alpha(T)$	$\mu(T)/T$	$\alpha(T)$	$\mu(T)/T$
5.3	0.142(2)	3.53(3)	0.135(2)	3.40(3)
5.4	0.102(3)	4.06(11)	0.097(3)	3.90(10)
5.6	0.082(1)	4.85(1)	0.097(1)	5.71(1)
5.8	0.058(1)	5.04(1)	0.071(1)	5.97(1)

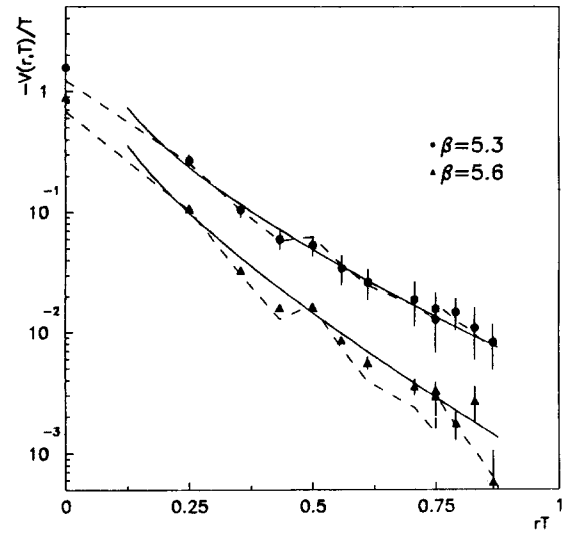

Fig. 3. Comparison between lattice (dashed lines) and continuum (full lines) fits to the potential measured on a $12^3 4$ lattice at $\beta = 5.3$ and 5.6.

[#1] Periodic boundary conditions have, of course, been taken into account.

Table 2
Screening masses $\mu_R(T)$ as obtained from eq. (7).

β	$\mu_1(T)/T$	$\mu_2(T)/T$
5.3	3.74(55)	3.26(90)
5.4	4.22(45)	3.88(80)
5.6	4.75(10)	4.77(67)
5.8	5.05(13)	3.87(85)

masses obtained from ratios of the potential at distances R and $R+1$

$$\mu_R = \ln\left(\frac{R}{R+1}\frac{V(R,T)}{V(R+1,T)}\right). \quad (7)$$

Results for $R=1$ and 2 are summarized in table 2. In general these quantities have large errors. However, the good agreement with the screening masses obtained from our fits shows that the errors are probably overestimated. Except for the largest coupling the screening masses obtained this way are roughly R independent ($\mu_1 \simeq \mu_2$). This also justifies our Debye-screened Coulomb ansatz, eq. (5).

Similar to the analysis in the pure gauge sector we find that the coupling constant $\alpha(T)$ decreases with increasing temperature. In fact, the decrease in compatible with $\alpha(T) \sim 1/T$. For the screening mass we find a substantially larger value than in the pure gauge sector. At large values of β ($\sim$ temperature) we obtain for the screening mass $\mu \simeq 5T$. This is to be compared with the value found in the pure SU(3) gauge theory, $\mu \simeq 3T$ [2,4]. Close to T_c the screening mass decreases substantially. However, it is still larger than in the pure gauge sector at comparable temperatures ($T \simeq 1.2T_c$). Qualitatively this agrees with our expectations: At a given temperature there are more partons around that can contribute to the screening of the static fermion sources. The effect seems, however, to be stronger than expected on the basis of the perturbative relation given in eq. (2).

Let us finally discuss other thermodynamic observables of interest in the plasma phase. In table 3 we summarize our results for the gluonic and fermionic parts of the energy density as well as the Polyakov loop expectation values [#2].

As can be seen finite-size effects coming from the finite spatial extent of the lattice are small for these observables. This is in agreement with results from weak coupling perturbation theory [15,16] which indicate only a weak dependence on the spatial lattice size. For our case, i.e. two light flavours of mass $ma=0.025$, we obtain for the gluonic and fermionic parts of the energy density the perturbative results

$$\epsilon_G/T^4 = 7.36 + 15.11/\beta,$$
$$\epsilon_F/T^4 = 12.84 - 4.41/\beta \quad (8)$$

on an $8^3 4$ lattice, and

$$\epsilon_G/T^4 = 7.72 + 12.91/\beta,$$
$$\epsilon_F/T^4 = 12.25 - 5.46/\beta \quad (9)$$

on a $12^3 4$ lattice. In figs. 4a and 4b we compare these perturbative relations with our Monte Carlo data. As can be seen the agreement of the fermionic part of the

[#2] We determine the gluonic part of the energy density only from the difference of space- and time-like plaquettes. The small corrections coming from terms proportional to derivatives of the coupling g^2 have been neglected. Similarly we leave out the term proportional to the quark mass in the definition of the fermionic part of the energy density. For detailed definitions see for instance ref. [11] and references therein.

Table 3
Summary of results for the gluonic (ϵ_G) and fermionic (ϵ_F) parts of the energy density on the $8^3 4$ and $12^3 4$ lattices. We also give the Polyakov loop expectation value ($\langle L \rangle$) and the chiral condensate ($\langle \bar{\chi}\chi \rangle$).

Lattice	β	$\epsilon_G a^4$	$\epsilon_F a^4$	$\langle L \rangle$	$\langle \bar{\chi}\chi \rangle$
$8^3 4$	5.28	0.0123(46)	0.0081(5)	0.1402(186)	0.7271(95)
	5.3	0.0445(29)	0.0323(3)	0.4410(188)	0.3588(172)
	5.6	0.0626(33)	0.0414(2)	0.7673(85)	0.1230(8)
$12^3 4$	5.3	0.0459(31)	0.0348(2)	0.4835(95)	0.2933(97)
	5.4	0.0582(26)	0.0388(2)	0.6045(64)	0.1770(19)
	5.6	0.0584(15)	0.0408(1)	0.7557(37)	0.1232(3)
	5.8	0.0564(23)	0.0415(1)	0.8694(50)	0.1045(2)

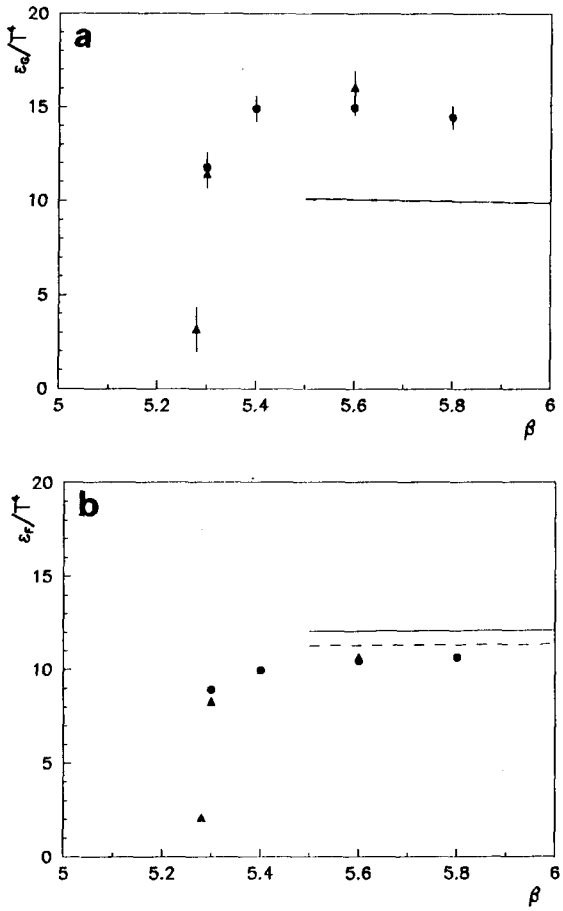

Fig. 4. The gluonic (a) and fermionic (b) parts of the energy density versus β measured on $12^3 4$ (●) and $8^3 4$ (▲) lattices. In (b) errors are of the size of the symbols. The curves show the perturbative results given in eq. (9) (full lines) and eq. (8) (dashed lines). These two curves coincide in (a).

energy density with the perturbative result is quite good already for $\beta = 5.4$, i.e. close to T_c. The gluonic part, however, overshoots the perturbative result considerably. This has been noted before in the case of four-flavour QCD [17] and is present also in simulations of SU(2) gauge theory with staggered fermions [16]. In fact the $O(1/\beta)$-correction to the finite lattice perturbative result for the gluonic energy density has the opposite sign compared to the perturbative result for the continuum theory [16]. This originates in the small temporal extent, N_τ, of the lattice by which all higher Matsubara frequencies are eliminated. Much larger lattices are needed to get agreement between perturbative calculations on the lattice and in the continuum. We thus have to conclude that the observed overshooting of the ideal gas limit in the gluonic sector may not be a physical effect. Simulations on larger lattices will be needed to clarify this issue, but these will be difficult since the changes, comparing $8^3 4$ and $12^3 4$, are small and the latter size already stretches current computer power for the fastest available fermion algorithms.

In conclusion, we find that including dynamical light fermions increases the Debye screening mass from $\mu \simeq 3T$ to $\mu \simeq 5T$. Finite-size effects are significant for the heavy quark potential in comparing $8^3 4$ with $12^3 4$ but small for global quantities such as the gluon energy density, so that the anomalously large value for this latter quantity remains unexplained.

The Monte Carlo simulations were performed on the Crays X-MP/48 at the HLRZ in Jülich, CERN and NCSA in Urbana-Champaign. We thank these computer centers for their cooperation.

References

[1] S. Nadkarni, Phys. Rev. D 33 (1986) 3738; D 34 (1986) 3904.
[2] T.A. DeGrand and C.E. DeTar, Phys. Rev. D 34 (1986) 2469.
[3] K. Kanaya and H. Satz, Phys. Rev. D 34 (1986) 3193.
[4] N. Attig et al., Polyakov loop correlations in Landau gauge and the heavy quark potential, CERN preprint CERN-TH.4955/88 (January 1988).
[5] J. Engels, F. Karsch and H. Satz, A finite size analysis of the heavy quark potential in a deconfining medium, CERN preprint CERN-TH.5024/88 (April 1988).
[6] R.V. Gavai, M. Lev, B. Petersson and H. Satz, Phys. Lett. B 203 (1988) 295.
[7] T. Matsui and H. Satz, Phys. Lett. B 178 (1986) 416.
[8] F. Karsch, M.T. Mehr and H. Satz, Z. Phys. C 37 (1988) 617.
[9] S. Duane, Nucl. Phys. B 257 [FS14] (1985) 652.
[10] S. Gottlieb et al., Phys. Rev. D 35 (1987) 2531.
[11] S. Gottlieb et al., Phys. Rev. D 35 (1987) 3972.
[12] S. Gottlieb et al., Phys. Rev. Lett. 59 (1987) 1513.
[13] C.B. Lang and C. Rebbi, Phys. Lett. B 115 (1982) 137; A. Hasenfratz et al., Z. Phys. C 25 (1984) 191.
[14] H.Th. Elze, K. Kajantie and J. Kapusta, Helsinki preprint HU-TFT-88-1 (January 1988).
[15] F. Karsch and U. Heller, Nucl. Phys. B 251 [FS13] (1985) 254.
[16] F. Karsch and U. Heller, Nucl. Phys. B 258 (1985) 29.
[17] F. Karsch, J.B. Kogut, D.K. Sinclair and H.W. Wyld, Phys. Lett. B 188 (1987) 353.